

# Numerical analysis of intralaminar damage evolution on various composite laminates

**I Hudisteanu<sup>1</sup>, N Taranu, D N Isopescu, I-S Entuc, G Oprisan and D Ungureanu**  
“Gheorghe Asachi” Technical University of Iasi, Faculty of Civil Engineering and Building Services, Department of Civil and Industrial Engineering, Blvd. Mangeron, No. 1, 700050, Iasi, Romania

E-mail: iulianahudisteanu@ce.tuiasi.ro

**Abstract.** The paper presents the numerical modelling of progressive damage distribution on the layers of various configurations of composite laminates (cross-ply, angle-ply, balanced laminate and quasi-isotropic laminate) under tensile loading. The purpose of the paper is to study the effect of the stacking sequence and fibre orientation angles on the damage propagation on multi-layered composites. These damage initiations do not necessarily imply a complete loss of structural integrity of the composite laminate. Additional load can be supported due to the stress redistribution over the fibres. A post-critical analysis is carried out, in order to analyse the integrity or the degradation state of the layers of composite laminates. The progressive failure analysis is performed in ANSYS Composite Prep/Post, to enable the investigation of damage initiation and damage evolution on each ply with various fibre orientations of the composite laminates. The intralaminar failure is initially detected based on a failure criterion and the post-critical analysis is evaluated based on a damage evolution law. The results are presented in terms of representative tensile displacements, which lead to damage initiation and damage evolution on the layers of the analysed composite laminates. Moreover, the laminas with different fibre orientations are investigated for progressive loading steps, from the first local failure to the total collapse. The obtained results show that the damages distribution on the plies of the composite laminates are strongly influenced by the fibre orientations, but also by the interaction with the other laminas and stacking sequence.

## 1. Introduction

Composite structures provide an alternative solution to traditional materials. Due to their convenient stiffness and strength properties combined with weight savings, they are used in a wide range of domains, such as aerospace, automotive and civil engineering applications. In the construction sector, composite materials are increasingly utilized in strengthening procedures for various structural elements and materials, such as concrete, timber and masonry [1-4]. Moreover, the fibre reinforced polymeric (FRP) composite materials used to improve the bearing capacity of the existing structural elements represent a sustainable environment solution, proven by the environmental impact parameters in literature [5].

The mechanical behaviour of composite materials is still an actual concern, due to its complexity given by the anisotropy and heterogeneity. The difficulty of failure prediction is increased in case of multi-layered composites, when other important parameters such as fibre orientation angle and stacking sequence are added. The necessity of predicting and tailoring the damage mechanisms in multi-layered composites, such as intralaminar and interlaminar failure modes, has led to recent



researches, to improve the understanding of the composites' behaviour [6-11]. The intralaminar failure mechanisms which may occur in a composite lamina when it is subjected to in-plane loads refer to the fibre rupture or breaking, matrix cracking, fibre buckling or kinking and matrix crushing [12].

The paper presents the numerical study of the intralaminar damage onset and damage evolution on the layers of different configuration composite laminates subjected to imposed tensile displacements. The main goal is to improve the understanding of the complex behaviour of multi-layered composites, by predicting the damage distributions with respect to the fibre orientation angle, stacking sequence, laminate configuration and loading direction.

## 2. Description of the analysed cases and theoretical background

Four types of symmetric specially orthotropic composite laminates are analysed, with the following configurations:  $[90/0/90]_2/(0)_2$ , cross-ply laminate,  $[(\pm 60)_3]_s$  angle-ply laminate,  $[0/15/30/45/90/-45]_s$  balanced laminate and  $[0/30/60/90/-60/-30]_s$  quasi-isotropic laminate, as shown in figure 1.

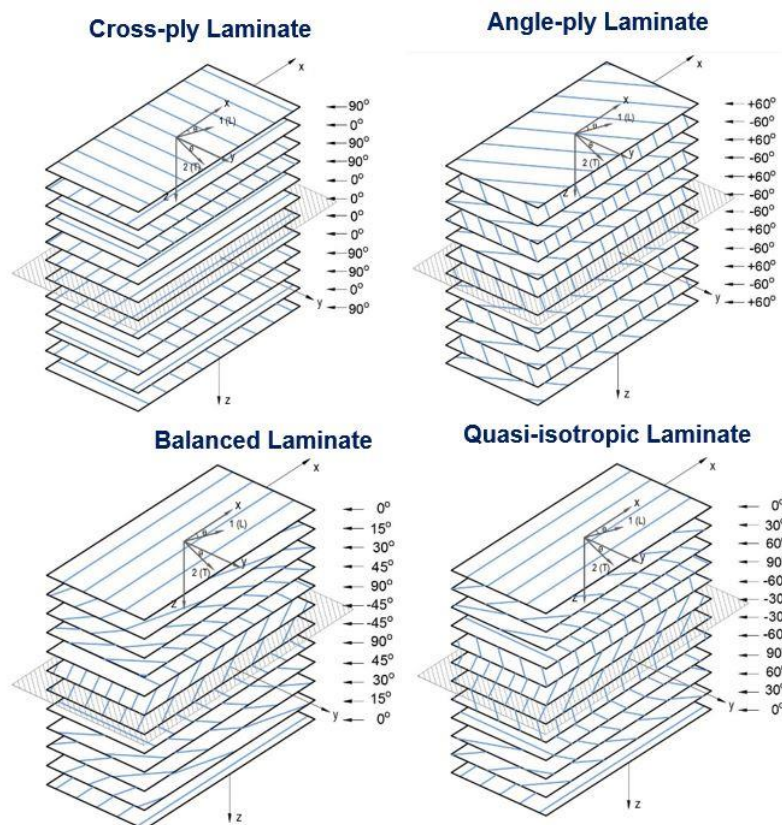


**Figure 1.** Stacking sequences of the analysed multi-layered composites.

The investigation of damage evolution is performed in ANSYS Composite Prep/Post, in order to enable the visualization of the damage occurrence on each ply with different fibre orientation angles. Since the intralaminar damage distributions are investigated, the numerical model of the multi-layered composites is defined using bi-dimensional finite elements, such as SHELL181 [13], which provides four nodes and six degrees of freedom at each node, figure 2.a. This finite element is well-suited for modelling thin and moderately-thick multi-layered composites, its degree of accuracy being related to the *First-Order Shear-Deformation Theory* (FOSDT), [14].

The four cases of composite laminates have the same total thickness of 3 mm (12 composite layers x 0.25 mm/layer) and the in-plane dimensions of 500 mm x 500 mm. The boundary conditions of the numerical model consist in fixed support at one end and in-plane tensile displacement in  $x$  direction at the opposite end.

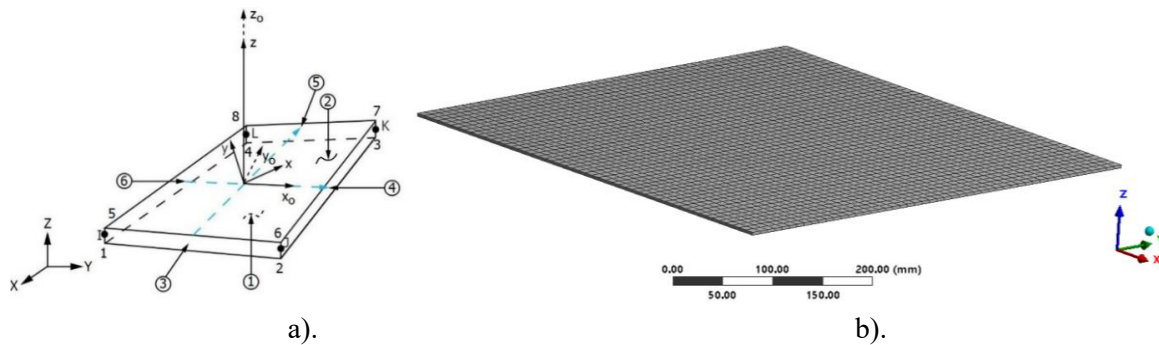


**Figure 2.** a). SHELL181 finite element used for the model; b) the mesh and geometry of the laminates.

The analysed multi-layered composites are made of S glass fibres embedded in an epoxy resin, with a fibre volume fraction of 60%. The mechanical properties of the composite lamina used in the numerical modelling are presented in table 1 [15].

**Table 1.** Mechanical properties of *S glass-epoxy* composite lamina\* [15].

$E_1$ [GPa]	$E_2$ [GPa]	$G_{12}$ [GPa]	$\nu_{12}$	$f_{1t}$ [MPa]	$f_{1c}$ [MPa]	$f_{2t}$ [MPa]	$f_{2c}$ [MPa]	$f_{12s}$ [MPa]
52.94	13.93	5.07	0.292	2836	1122	62.53	125.1	58.29

\*where:  $E_1$  and  $E_2$  are the longitudinal and transverse modulus, respectively;  $G_{12}$  - the shear modulus;  $\nu_{12}$  - the in-plane major Poisson's ratio;  $f_{1t}$  and  $f_{1c}$  are the longitudinal tensile and compressive strength;  $f_{2t}$  and  $f_{2c}$  are the transverse tensile and compressive strength, respectively;  $f_{12s}$  - the in-plane shear strength.

The intralaminar failure is initially detected based on a failure criterion and the post-critical analysis is evaluated based on a damage evolution law.

The failure criterion used in the paper is the maximum strains theory, equations (1), according to which the failure occurs when any of the specific strains along the principal material axes exceed the corresponding ultimate specific strains:

$$-\varepsilon_{1c} < \varepsilon_1 < \varepsilon_{1t}; \quad -\varepsilon_{2c} < \varepsilon_2 < \varepsilon_{2t}; \quad -\gamma_{12s} < \gamma_{12} < \gamma_{12s} \quad (1)$$

where:  $\varepsilon_{1t}$  and  $\varepsilon_{1c}$  are the ultimate specific strains at longitudinal tension and compression, respectively;  $\varepsilon_{2t}$  and  $\varepsilon_{2c}$  - the ultimate specific strains at transverse tension and compression, respectively;  $\gamma_{12s}$  - the ultimate specific strain at shear in (12) plane.

The effective maximum strains ( $\varepsilon_1, \varepsilon_2, \gamma_{12}$ ) with respect to the principal material axes, for an equivalent longitudinal stress  $\sigma_x$ , are expressed as following:

$$\varepsilon_1 = \frac{\sigma_x}{E_1} (\cos^2 \theta - \nu_{12} \sin^2 \theta); \quad \varepsilon_2 = \frac{\sigma_x}{E_2} (\sin^2 \theta - \nu_{21} \cos^2 \theta); \quad \gamma_{12} = \frac{\sigma_x}{G_{12}} \sin \theta \cos \theta \quad (2)$$

where:  $\sigma_x$  is the normal stress along the global x axis;  $\theta$  is the fibre orientation angle.

A linearly elastic damage evolution law available in ANSYS is used in order to study the effect of fibres orientation and stacking sequence on the damage propagation on each layer of various configurations of composite laminates.

The progressive damage analysis used in this paper is based on a gradual degradation model of the material stiffness, which enables a gradual reduction of the material properties, related to specific modes of failure [16]. This model approach available in ANSYS is a generalisation of the work of Davila and Camanho [17, 18]. According to the gradual degradation model, the material behaves

elastically until the onset of damage occurs, followed by a softening of the material or a damage phase, figure 3, when the stiffness material matrix is progressively reduced. The damage evolution law refers to the material evolution law, after the initiation of damage has occurred. The constitutive equations used for the prediction of the post-damage degradation of the material have the following form [13, 17-19]:

$$\tilde{\sigma} = [D] \cdot \varepsilon \quad \text{and} \quad \sigma = [D]_d \cdot \varepsilon, \quad (3)$$

where:  $\tilde{\sigma}$  represents the effective stress (in the undamaged domain),  $\sigma$  is the nominal stress (the average stress, measured in both damaged and undamaged domains),  $\varepsilon$  is the elastic strain,  $[D]$  represents the undamaged stiffness matrix, and  $[D]_d$  is the damaged stiffness matrix.

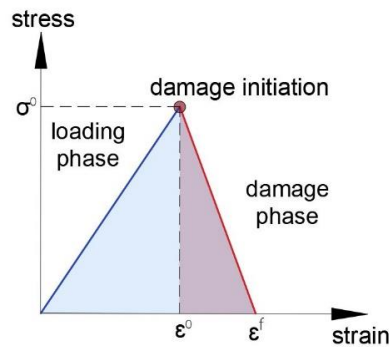


**Figure 3.** Constitutive model for a linearly softening material.

The damaged stiffness matrix is affected by the scalar damage variable  $d$ , which is introduced to take into account the material damage. In other words, the damage can be associated with a reduction in material properties. For an orthotropic composite material, the damaged stiffness matrix has the following general form:

$$[D]_d = \begin{bmatrix} \frac{s_{11}}{(1-d_f)} & s_{12} & s_{13} & 0 & 0 & 0 \\ s_{12} & \frac{s_{22}}{(1-d_m)} & s_{23} & 0 & 0 & 0 \\ s_{13} & s_{23} & \frac{s_{33}}{(1-d_m)} & 0 & 0 & 0 \\ 0 & 0 & 0 & \frac{s_{44}}{(1-d_s)} & 0 & 0 \\ 0 & 0 & 0 & 0 & \frac{s_{55}}{(1-d_s)} & 0 \\ 0 & 0 & 0 & 0 & 0 & \frac{s_{66}}{(1-d_s)} \end{bmatrix}^{-1}, \quad (4)$$

where:  $d_f$ ,  $d_m$  represent the damage variables for fibers and matrix, respectively;  $d_s$  is the shear damage variable;  $S_{ij}$  are the terms of the compliance matrix of the undamaged material.

For a plane stress state, the damaged stiffness matrix for thin fibre reinforced composites can be expressed with respect to the elastic engineering constants, as follows:

$$[D]_d = \frac{1}{A} \begin{bmatrix} (1-d_f) \cdot E_1 & (1-d_f)(1-d_m) \cdot \nu_{21} \cdot E_1 & 0 \\ (1-d_f)(1-d_m) \cdot \nu_{12} \cdot E_2 & (1-d_m) \cdot E_2 & 0 \\ 0 & 0 & A \cdot (1-d_s) \cdot G_{12} \end{bmatrix}, \quad (5)$$

with  $A = 1 - (1-d_f)(1-d_m) \cdot \nu_{12} \cdot \nu_{21}$ .

Depending on the state of loading (tensile stresses or compressive stresses), four different damage modes are considered, such as fibre tension ( $d_{ft}$ ), fibre compression ( $d_{fc}$ ), matrix tension ( $d_{mt}$ ) and matrix compression ( $d_{mc}$ ), therefore their corresponding damage variables are expressed as follows:

$$d_f = \begin{cases} d_{ft}, & \text{if } \sigma_1 \geq 0 \\ d_{fc}, & \text{if } \sigma_1 < 0 \end{cases} \quad \text{and} \quad d_m = \begin{cases} d_{mt}, & \text{if } \sigma_2 \geq 0 \\ d_{mc}, & \text{if } \sigma_2 < 0 \end{cases} \quad (6)$$

$$d_s = 1 - (1 - d_{ft})(1 - d_{fc})(1 - d_{mt})(1 - d_{mc}).$$

These damage variables range from 0 (undamaged material status) to 1 (completely damaged material status).

### 3. Intralaminar damage investigations. Results discussion

The purpose of the paper is to detect the damage onset on the layers of the composite laminates subjected to in-plane tensile loads and to investigate the effect of the fibres orientation and stacking sequence on the intralaminar damage evolution modes.

For each analysed composite laminate, the damage status is first presented for a representative tensile displacement (figures 4, 5, 7, 9, 11), selected so that the damages can be localized on each lamina and the differences between the layers, but also between the considered laminates can be noticed.

A real interest is focused on the effect of the fibre orientation angles on the intralaminar damage evolution on the layers of the composite laminate. Because a single tensile displacement is not sufficient to describe the damage evolution, the laminated composites are progressively loaded and representative tensile displacements are selected so that an accurate distribution of the degradations from the initiation to the complete damage can be shown.

#### 3.1. Cross-ply laminate

Figure 4 shows the intralaminar damages on the layers of the analysed configuration of the **cross-ply laminate**, subjected to in-plane longitudinal traction, for a tensile displacement  $\Delta = 2.3$  mm. This loading step was selected from preliminary numerical simulations in order to illustrate the moment when the layers oriented at  $90^\circ$  are characterised by significant degradations. Moreover, it can be observed that the layers with the fibres orientation angles of  $0^\circ$  are still not affected.

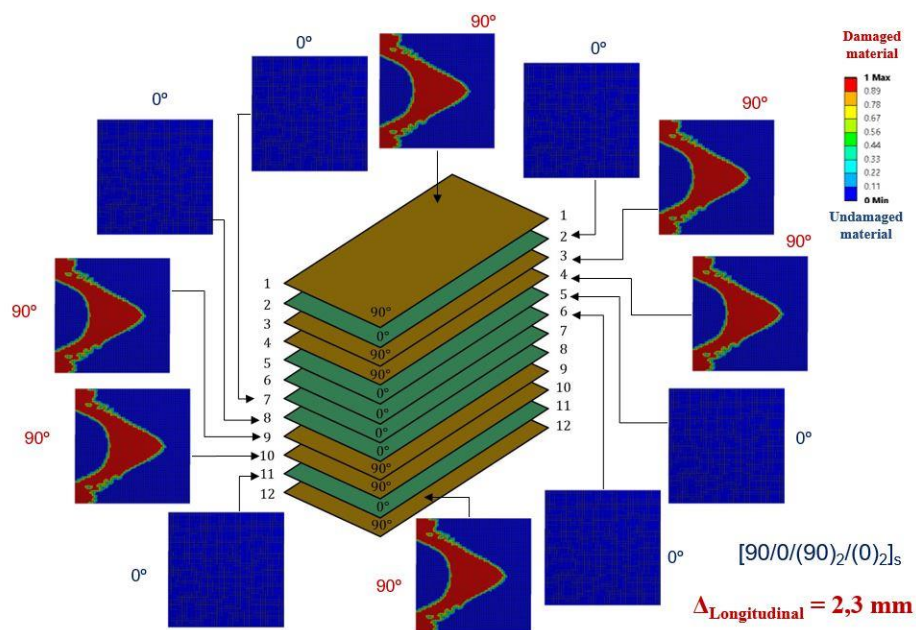
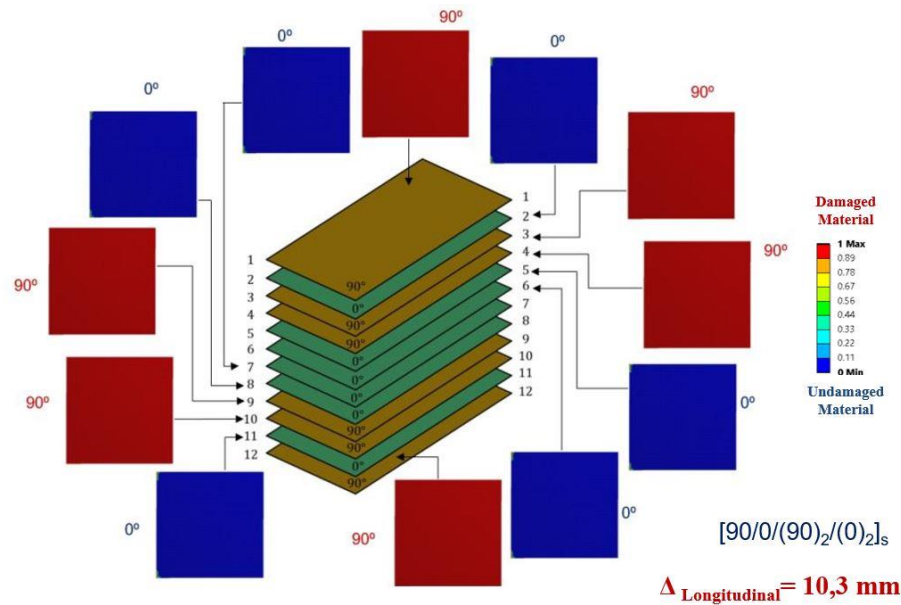


Figure 4. Intralaminar damages on the layers of the **cross-ply laminate** ( $\Delta_{\text{Longitudinal}} = 2.3$  mm).

An imposed displacement equal to 10.3 mm provides the damage onset on the layers orientated at 0°, while the laminas with 90° fibres orientations are completely damaged, figure 5.



**Figure 5.** Intralaminar damages on the layers of the *cross-ply laminate* ( $\Delta_{\text{Longitudinal}}=10.3$  mm).

Progressive damage analysis is carried out to identify the behaviour of the layers with 90° and 0° fibres orientations of the cross-ply laminate subjected to longitudinal traction. The laminate is investigated for progressive tensile displacements, corresponding to the damage initiation until the complete damage occurs. Figure 6 presents the intralaminar damages evolution for the layers with 90° and 0° fibres orientations and the mode of propagation up to a total collapse.

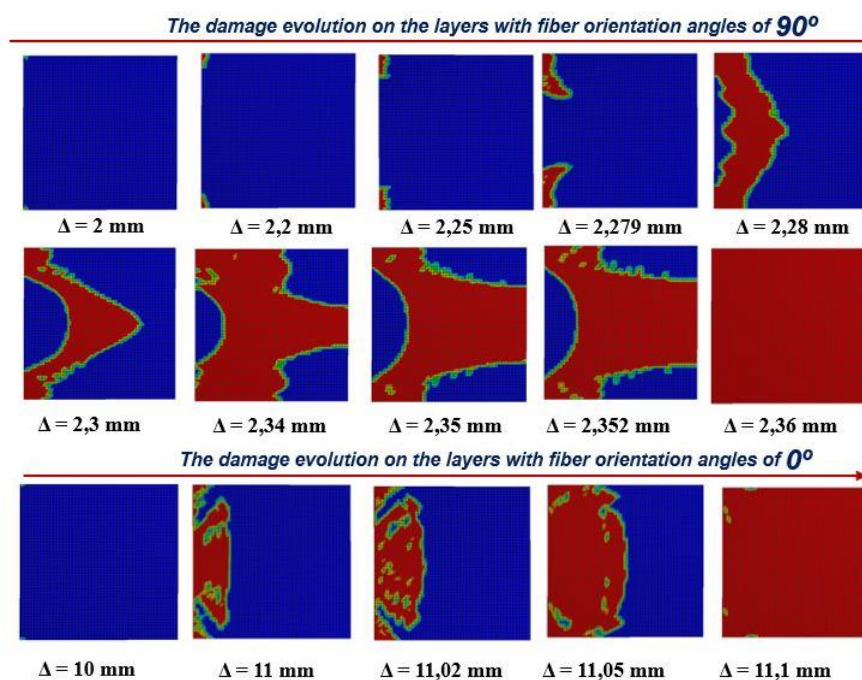


**Figure 6.** Progressive damage distributions on the layers of the *cross-ply laminate*.

It can be noticed that the layers oriented at  $90^\circ$  display a highly accelerated failure and the tensile imposed displacements corresponding to the damage onset and the complete collapse are ranging between 2 mm and 2.36 mm, which leads to a brittle fracture of these laminas.

For the layers with the fibres orientation angles of  $0^\circ$ , the failure is very gradual and the damage initiation occurs for  $\Delta = 10$  mm, up to a final rupture of  $\Delta = 11.1$  mm.

The fracture of the cross-ply laminate is characterised by two failure steps, up to a tensile displacement of 2.36 mm, and the only layers undertaking longitudinal stresses are the laminas oriented at  $0^\circ$ . The degradations are enlarged from the fixed end to the loaded one, for both  $0^\circ$  and  $90^\circ$  oriented laminas, yet the way the intralaminar damages propagate is strongly influenced by the fibres orientations.

### 3.2. Angle-ply laminate

The intralaminar damages on the layers of the *angle-ply laminate* under longitudinal traction are presented for a single loading step of  $\Delta = 3$  mm, figure 7, because insignificant differences are noticed between  $+60^\circ$  and  $-60^\circ$  oriented plies due to the symmetry of laminas orientations with respect to the loading direction.

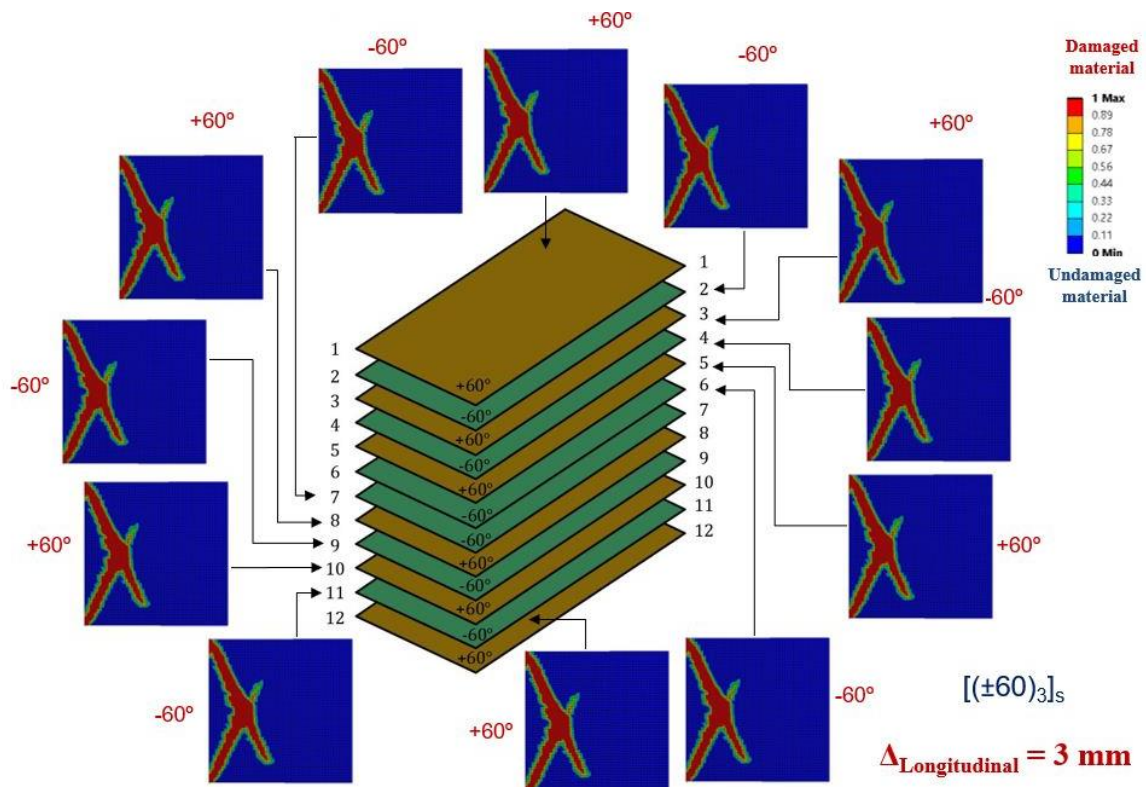


**Figure 7.** Intralaminar damages on the layers of the *angle-ply laminate* under longitudinal traction.

For the identification of the damage evolution on the  $\pm 60^\circ$  laminas, progressive tensile displacements are imposed, corresponding to the interval of 2 mm - 20 mm, figure 8. Since the distribution of the damages are almost similar, there are selected only the laminas with  $+60^\circ$  fibres orientations.

Compared to the cross-ply laminate, the angle-ply multi-layered composite elements withstand an almost double tensile displacement. Although the tensile strength of the laminas oriented at  $\pm 60^\circ$  is lower than that of laminas with the fibres arrangement parallel to the direction of loading, the advantage of the analysed angle-ply laminate is that all the layers resist until the final failure. The

inconvenient aspect of this situation consists in the sudden loss of carrying capacity and, therefore, a catastrophic failure of the angle-ply laminate.

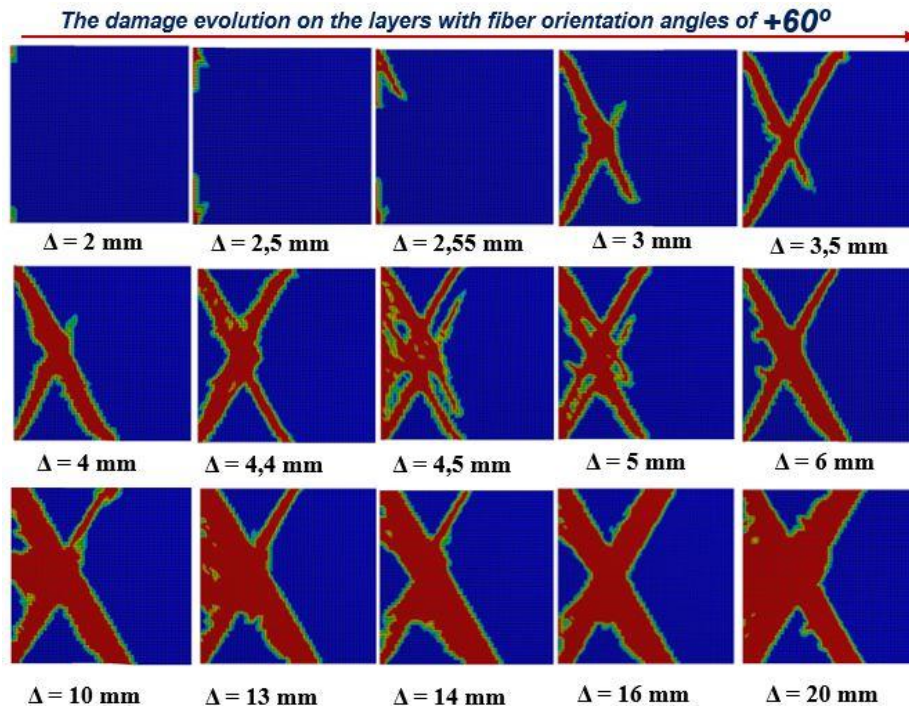


**Figure 8.** Progressive damage distributions on the layers of the *angle-ply laminate*.

The damage onsets are located in the corners of the fixed end and their distributions propagate to the loaded end in an *X* shape.

### 3.3. *Balanced laminate*

For the *balanced laminate*  $[0/15/30/45/90/-45]_s$ , a representative loading stage is selected for a tensile displacement of  $\Delta = 11.1$  mm, figure 9, which illustrates the intralaminar damage occurrence on every component layer.

At this stage, the laminas with fibre orientation angles of  $90^\circ$  are completely damaged, while the plies whose fibres are parallel to the loading direction present damage onset. Significant degradations and approximately similar damage distributions can be noticed on the layers oriented at  $\pm 45^\circ$  and  $30^\circ$ . For the plies with the fibre orientation angles of  $15^\circ$ , a local central failure is identified.

In general, the first ply failure occurrence might not have a major importance on the structural capacity of the multi-layered composites. Since the layers of the composite laminates continue to fail, the laminate structural integrity is compromised and the element becomes vulnerable to complete failure. When the multi-layered composites have a balanced behaviour with respect to the fibres arrangement and orientation, they are less exposed to a catastrophic failure.

The investigation of the damage evolution is realized for every different oriented layer of the balanced laminate, from the damage onset to the complete collapse, figure 10. The sequence of the damaged layers, the number of the plies that are fractured simultaneously and their specific mode of damage evolution can be observed.

The investigation of the damage behaviour for the layers oriented at  $90^\circ$ , from the initiation to the complete damage, is performed for displacements with values ranging from  $\Delta = 1.4$  mm to 2.7 mm.

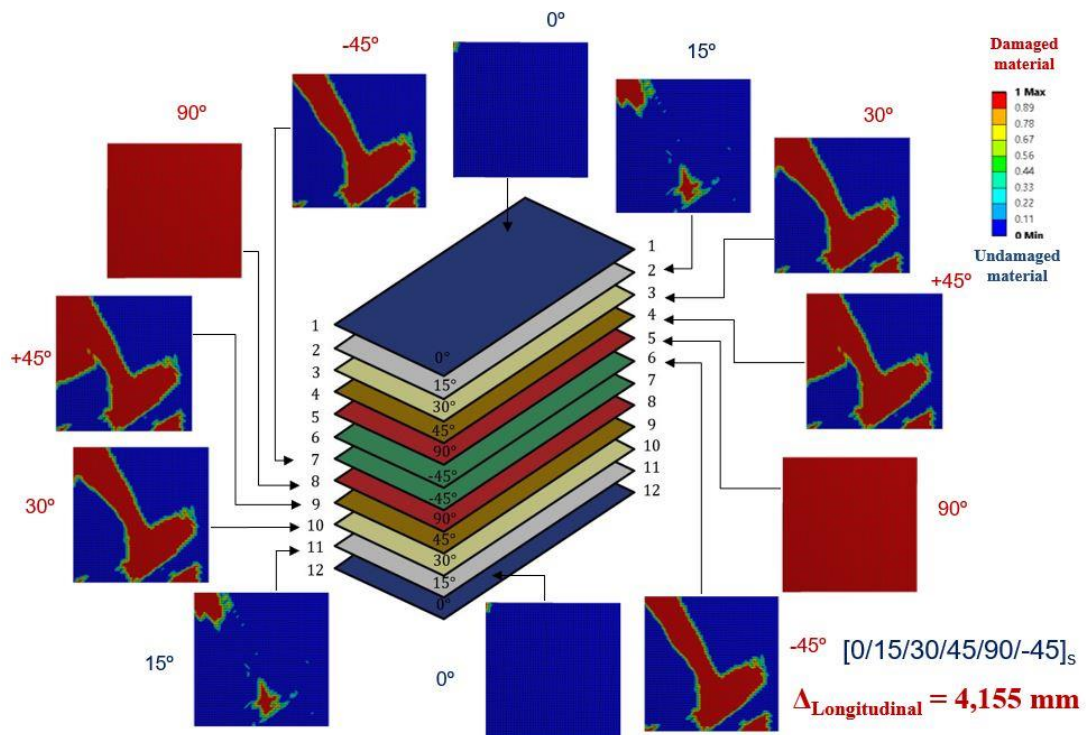


Figure 9. Intralaminar damages on the layers of the *balanced laminate* under longitudinal traction.

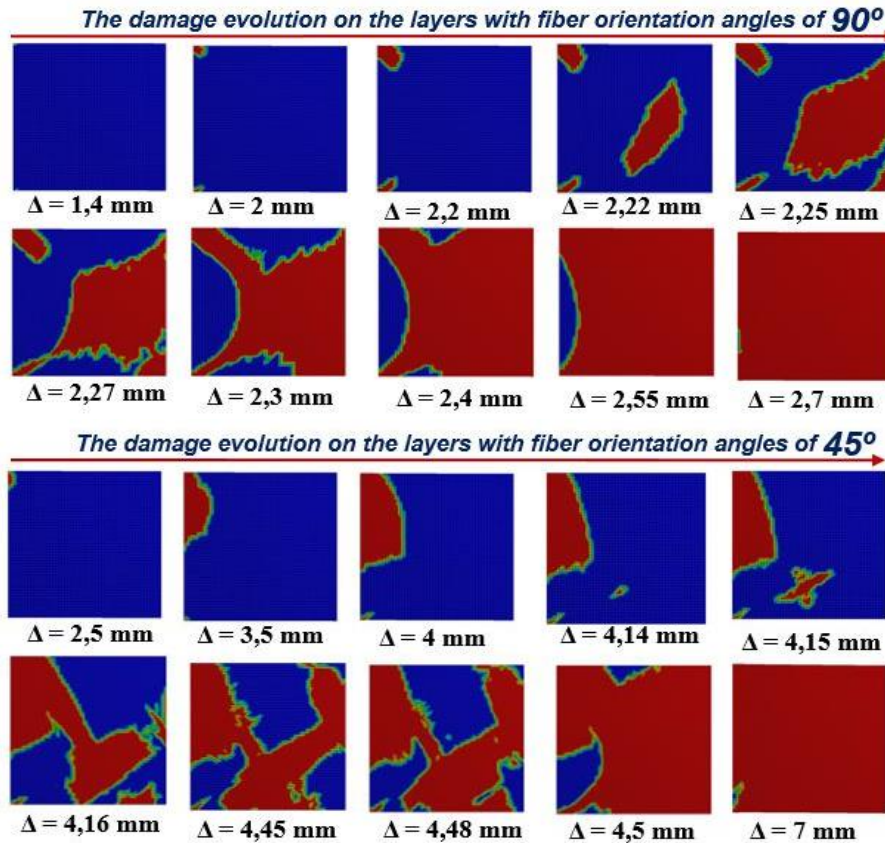
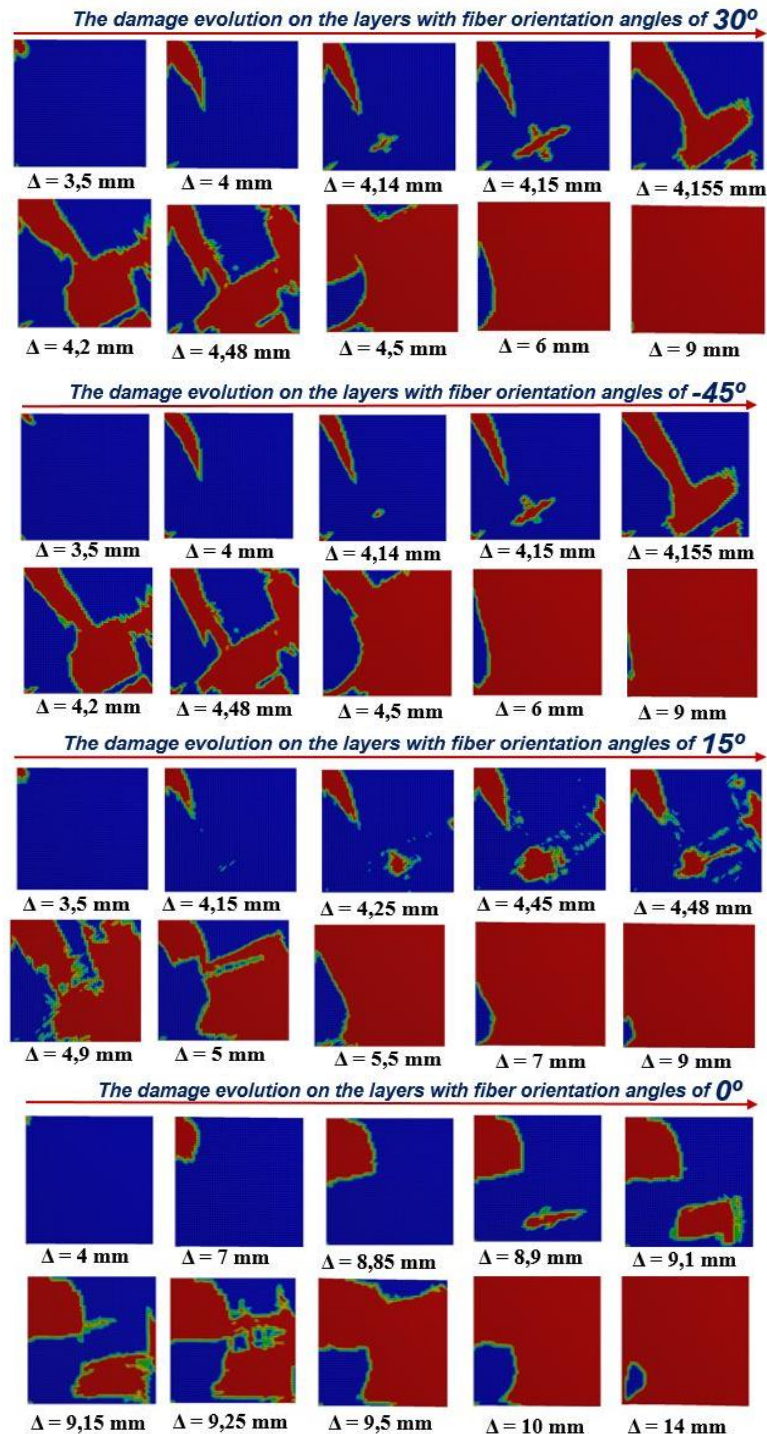


Fig. 10 continues next page



**Figure 10.** Progressive damage distributions on the layers of the *balanced laminate*.

The intralaminar degradations distribution is different compared to the damages obtained for the same orientation, in the case of the cross-ply laminate. Therefore, interaction with the other layers and the stacking sequence influence the overall mechanical behaviour and the intralaminar damage evolution mode.

For the layers oriented at  $+45^\circ$ , the damage evolution is analysed for displacements with values ranging from  $\Delta = 2.5$  mm to 7 mm, while the plies with fibres orientation angles of  $30^\circ$ ,  $-45^\circ$  and  $15^\circ$

are studied for the same interval of progressive displacements,  $\Delta = 3.5 - 9$  mm. Similar damage evolution mode can be noticed for the laminas oriented at  $\pm 45^\circ$  and  $30^\circ$ , while for the plies oriented at  $15^\circ$ , the degradations distribution is quite different.

The state of degradation of several laminas compared to the other layers from the balanced laminate can be analysed in figure 10, with respect to the imposed values of the displacements. Therefore, a tensile longitudinal displacement equal to 2.7 mm indicates the total collapse of the  $90^\circ$  oriented layers, while for the plies with fibre orientation angles of  $45^\circ$ , this loading stage represents the damage onset. For the laminas oriented at  $0^\circ$ , the initiation of damage occurs at  $\Delta = 4$  mm, while on the rest of the layers, enlarged damages are noticed. Moreover, the sequence of the plies failure can be established based on the damage status of each lamina and their corresponding failure displacements, such as:  $90^\circ$ ,  $+45^\circ$ ,  $30^\circ$ ,  $-45^\circ$ ,  $15^\circ$  and  $0^\circ$ .

Since the damage evolution mode for the cross-ply and angle-ply laminate follow a continuous path to the fixed end to the loaded one, in case of the balanced laminate, the damage onset is detected also on the supported end, but then local failure occurs in the central areas. These locally detected damages evolve towards the loaded end of the laminate and also merge in the opposite direction with the initial degradation. This mode of propagation of the damage can be explained by the balanced nature of the composite laminate, which could determine a redistribution of the in-plane stresses, due to its configuration. This damage distribution law is valid for each layer of the analysed balanced laminate.

### 3.4. Quasi-isotropic laminate

Figure 11 shows the intralaminar damages on the layers of the *quasi-isotropic laminate* loaded with a tensile displacement  $\Delta = 3.3$  mm, selected so that the degradations can be visible on the layers oriented at  $90^\circ$  and  $\pm 60^\circ$ , while the plies with the fibres orientation at  $\pm 30^\circ$  describe the damage onset.

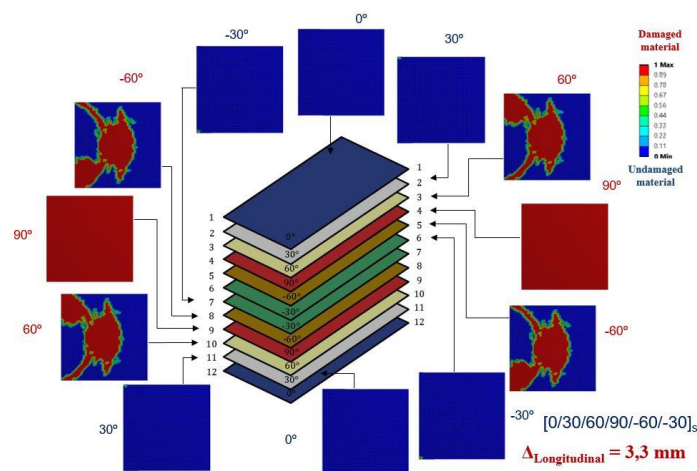


**Figure 11.** Intralaminar damages on the layers of the *quasi-isotropic laminate*.

The sequence failure of the layers ( $90^\circ$ ,  $\pm 60^\circ$ ,  $\pm 30^\circ$  and  $0^\circ$ ) with respect to the damages and their corresponding tensile displacements can be observed in figure 12.

The group of laminas oriented in  $\pm 60^\circ$  and  $\pm 30^\circ$  directions show symmetrical evolution of damages with respect to the  $x$  direction. The progression of degradation is investigated for tensile displacements values ranging from 2 mm to 5 mm, in case of the layers oriented at  $+60^\circ$ , and for the laminas oriented to  $+30^\circ$ , for imposed displacements  $\Delta = 2.7$  mm - 8 mm, in order to identify the damage onset and the complete failure of the plies. For laminas with the fibres orientation of  $0^\circ$ , the initiation of degradation occurs for  $\Delta = 8$  mm, when the rest of the layers undergo a complete loss of carrying capacity.

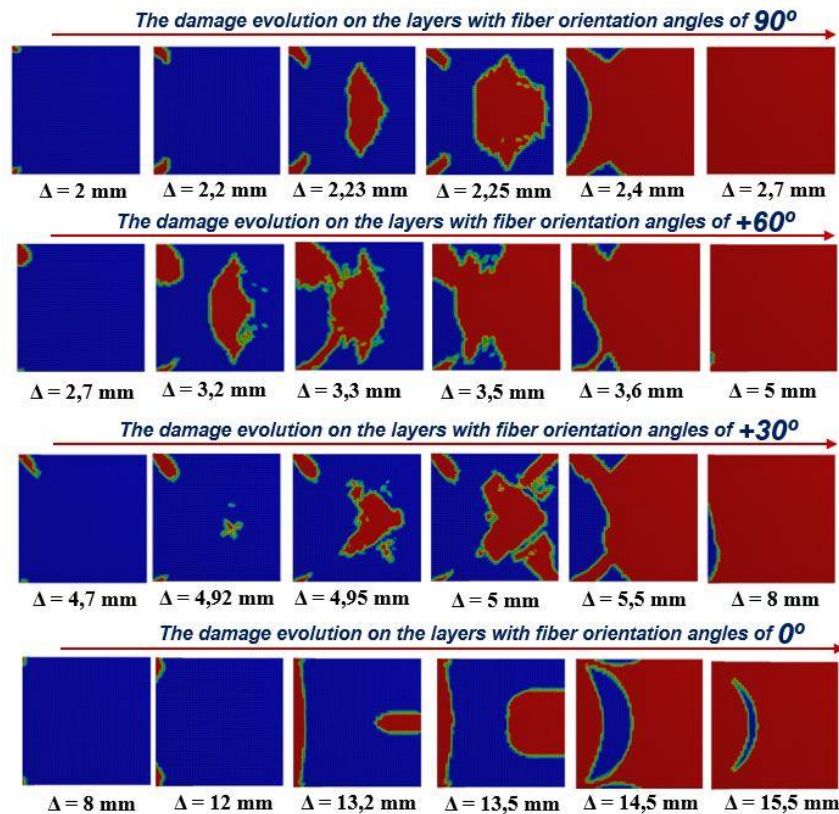


**Figure 12.** Progressive damage distributions on the layers of the *quasi-isotropic laminate*.

Central local damages are noticed for the layers with the fibre orientation angles of  $90^\circ$ ,  $\pm 60^\circ$  and  $\pm 30^\circ$ , which are spread in different directions and joined together to the initial one, followed by a complete extension towards the loaded end.

Unlike the cross-ply laminate, in case of balanced and quasi-isotropic laminates, the layers having the fibres parallel to the loading directions ( $0^\circ$  oriented laminas) show a different damage evolution mode. The degradations do not present a continuous extension from the fixed end to the loaded one, but local damages occur in the next vicinity to the damage onset, due to the redistribution of stresses.

The ultimate failure of the balanced and quasi-isotropic laminate occurs later (for  $\Delta = 14$  mm and  $\Delta = 15.5$  mm, respectively) than in the case of the cross-ply laminate ( $\Delta = 11.1$  mm), improving their structural behaviour through a gradual development of the damages.

#### 4. Conclusions

The paper presents the numerical assessment of the intralaminar damage onset and damage evolution for various configurations of composite laminates, as a consequence to imposed in-plane tensile displacements, in order to analyse the effect of fibre orientations on the damage propagations.

The obtained results revealed that the degradations distribution on the plies of the composite laminates are strongly influenced by the fibre orientations, but also by the interaction with the other laminas and stacking sequence.

The localization of damages occurrence and their tendency of evolution on the plies of the multi-layered composite is very important on predicting the complex intralaminar failure of composite laminates. Therefore, based on the progressive failure analysis, the gradual or the accelerated fracture of composite laminates can be described.

## 5. References

- [1] Oprisan G, Taranu N, Budescu M and Entuc I 2012 Structural behaviour of reinforced concrete beams strengthened by CFRP plate bonding *Rev Rom Mat* **42**(4) 387-398
- [2] Stanila O, Isopescu D and Taranu N 2014 Structural response of timber beams strengthened with advanced polymeric composite materials *Rev Rom Mat* **44**(4) 393-403
- [3] Verstryngge E, Wevers M, Ghiassi B and Lourenco P B 2016 Debonding damage analysis in composite-masonry strengthening systems with polymer- and mortar-based matrix by means of the acoustic emission technique *Smart Mat Struct* **25**(1) 015009
- [4] Taranu N, Oprisan G, Budescu M, Taranu G, Munteanu V and Bejan L 2010 Strengthening solutions based on textile composite for masonry structures *Proceedings of the 3rd International Conference on Advanced Materials and Systems* 149-154
- [5] Maxineasa S G, Taranu N, Bejan L, Isopescu D and Banu O M 2015 Environmental impact of carbon fibre-reinforced polymer flexural strengthening solutions of reinforced concrete beams *Int J Life Cycle Assess* **20** 1343-1358
- [6] Kang H, Shan Z, Zang Y and Liu F 2016 Progressive damage analysis and strength properties of fiber-bar composites reinforced by three-dimensional weaving under uniaxial tension *Compos Struct* **141** 264-281
- [7] Chen J F, Morozov E V and Shankar K 2014 Simulating progressive failure of composite laminates including in-ply and delamination damage effects *Compos Part A* **61** 185-200
- [8] Barbero E J and Shahbazi M 2017 Determination of Material Properties for ANSYS Progressive Damage Analysis of Laminated Composites *Compos Struct* **176** 768-779
- [9] Fischer S 2016 A Material Model for FE-Simulation of UD Composites *Appl Compos Mat* **23** 197-217
- [10] Liu P F, Gu Z P, Yang Y H and Peng X Q 2016 A nonlocal finite element model for progressive failure analysis of composite laminates *Compos Part B* **86** 178-196
- [11] Lee C S, Kim J H, Kim S K, Ryu D M and Lee J M 2015 Initial and progressive failure analyses for composite laminates using Puck failure criterion and damage-coupled finite element method *Compos Struct* **121** 406-419
- [12] Girão Coelho A M 2016 Finite Element Guidelines for Simulation of Delamination Dominated Failures in Composite Materials Validated by Case Studies *Arch Computat Methods Eng* **23** 363-388
- [13] ANSYS® Documentation, ANSYS, Inc
- [14] Reddy J N 2004 *Mechanics of laminated composite plates and shells. Theory and analysis. Second edition* (CRC Press, United States of America: Boca Raton)
- [15] Hudisteanu I, Taranu N, Isopescu D N, Bejan L, Axinte A and Ungureanu D 2017 Improving the mechanical properties of composite laminates through the suitable selection of the corresponding materials and configurations *Rev Rom Mat* **47**(2) 252-266
- [16] Riccio A, Costanzo C D, Gennaro P D, Sellito A and Raimondo A 2017 Intra-laminar progressive failure analysis of composite laminates with a large notch damage *Eng Fail Anal* **73** 97-112
- [17] Camanho P P and Dávila C G 2002 *Mixed-mode cohesion finite elements for the simulation of delamination in composite materials* (NASA/TM-2002-211737 2002) pp 1-37
- [18] Lapczyk J, Hurtado J A 2007 Progressive damage modeling in fiber-reinforced materials *Compos Part A* **38** 2333-41
- [19] Matzenmiller A, Lubliner J and Taylor R 1995 A constitutive model for anisotropic damage in fiber composites *Mech Mater* **20** 125-152